Journal of the European Ceramic Society **10** (1992) 205–211

Effect of Siloxane Infiltration of Green Samples on Properties of RBSN

S. Kleber

Fraunhofer-Einrichtung für Keramische Technologien und Sinterwerkstoffe, Winterbergstr. 28, O-8020 Dresden, Germany

&

H.-J. Weiss

Fraunhofer-Einrichtung für Werkstoffphysik und Schichttechnologie, Helmholtzstr. 20, O-8027 Dresden, Germany

(Received 30 March 1992; accepted 6 May 1992)

Abstract

It is demonstrated that the properties of reaction-bonded silicon nitride (RBSN) can be improved by addition of methylphenylsiloxane. When used as an auxiliary substance for granulating and pressing, it brings about higher density. Infiltration of the green samples by siloxane and subsequent pyrolysis produces a residue which changes the pore size distribution, with favourable effects on hardness and Young's modulus of the nitrided samples.

Es wird nachgewiesen, daß die Eigenschaften von RBSN durch Zugabe von Methylphenylsiloxan verbessert werden können. Bei Verwendung als Granulier- und Presshilfsmittel führt das Siloxan zu höherer Dichte. Infiltration der Grünkörper mit Siloxan und anschließende Pyrolyse ergibt einen Rückstand, der die Porengrößenverteilung so verändert, daß sich günstige Auswirkungen auf Härte und Elastizitätsmodul der nitridierten Proben ergeben.

Cet article rapporte l'amélioration des propriétés du RBSN après addition de méthylphénylsiloxane. Ce dernier, utilisé en tant que substance auxiliaire pour faciliter la granulation et le pressage de la poudre contribue à une meilleure densification. L'infiltration du siloxane dans l'échantillon cru, suivie par une pyrolyse produit un résidu qui change la distribution de la taille des pores avec un effet favorable sur la dureté et sur le module de Young des échantillons nitrurés.

1 Introduction

The good processibility of polysiloxanes suggests their use as auxiliary substances for granulating, pressing, sintering and infiltration. Their use in processing of structural ceramics has the essential advantage that they need not be completely removed in the process because their residue after thermal decomposition forms an additional phase which is compatible with the main components of the material and thus may be used for modification of the material properties. Because of these and other advantages, the use of precursors containing Si in ceramic processing has been a subject of investigation for some time. In addition to their use as auxiliary substances for moulding[1] they are used for sealing, coating, joining and reinforcing of ceramics.[2]

Controlled pyrolysis by addition of reactive fillers such as Ti, Cr, Zr or B in the AFCOP (active filler controlled pyrolysis) process is a promising novel way for the production of thin-walled monolithic structural ceramics.[3] Variation of type, composition, and properties of precursors provides a large field of parameters for optimizing the processing technology and modifying the mechanical and physical properties. The present paper concerns the use of low-polymer methylphenylsiloxane as an auxiliary substance in the production of reaction-bonded silicon nitride (RBSN).

RBSN is a suitable model substance for investigations in processing technology because of its simple

Journal of the European Ceramic Society 0955-2219/92/$5.00

relations between structure and properties. A decrease of both maximum flaw size and width of flaw size distribution is expected to be achievable by various mechanisms such as filling of pores, rounding off the edges of flaws or forming bridges across them. As a consequence there should be favourable influences on hardness, Weibull number, strength and fracture toughness.

2 Siloxane as an Auxiliary Substance for Granulating and Pressing

The investigations were carried out with two silicon powders labelled Sil and S/M (Fig. 1). The powder S/M was derived from milling dust formed in the production process of high-grade silicon for chips. The dust was fractionized according to grain size. The fractions were mixed in such proportion as to obtain a wide distribution with fractions of small grain sizes larger than usual. This leads to a configuration of larger particles embedded in a matrix of smaller ones, which is a necessary condition for optimal packing in the green state.

Unlike the powder S/M originating from ball milling, the commercial powder Sil is produced by means of a jet mill. Its mean grain size is much smaller, and its size distribution is narrow and nearly symmetric. This distribution as well as the more rounded grain shape are the causes for lower green density (Table 1). In order to facilitate pressing, a granulate with 10 wt% methylphenylsiloxane (Chemiewerk Nünchritz, Nünchritz, Germany) was prepared. The silicon powder was suspended in a 50% ethanol solution of silicon resin, dispersed by a RS ultrafine pulverizer, then dried and granulated by means of a spray granulator. After evaporation of the ethanol, the grains are covered and bound into granules by the siloxane.

In the die forming process the granules must deform under the pressure, otherwise the granule

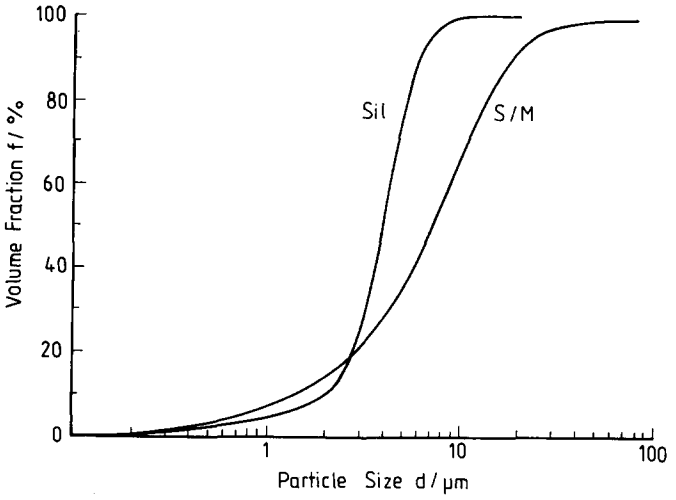

Fig. 1. Particle size distribution of silicon powders S/M and Sil.

structure would be found within the green sample. This would not be removed by sintering and thus would form large defects responsible for low strength. Deforming granules result in good performance of the granulate with respect to pressing and densification. Even after storing the granulate for one year, the green density of the samples did fit to the curves of Fig. 2. With a given powder type, the green density depends on pressure, pressing conditions, fraction and type of auxiliary substance. The green density increases by addition of methylphenylsiloxane as seen in Fig. 2. It is also seen that a 30% higher pressing rate yields considerably higher green density despite the lower applied pressure, which is rather remarkable and useful: lower pressure means less tool wear and lower cost. The advantageous influence of the low-molecular polymethylphenylsiloxane is thought to be due to its anti-adhesive and shear rate dependent rheological properties, although this hypothesis has not been substantiated by measurement so far.

For extended investigations, rods of size $4 \times 5 \times 60\,mm^3$ were prepared under 250 MPa. As another advantage, sufficient stability of the green samples

Table 1. Properties of RBSN made from silicon powders S/M and Sil with addition of low molecular polymethylphenylsiloxane as an auxiliary substance

	Powder type			
	S/M	*Sil*	*S/M*	*Sil*
Powder				
Average particle size (µm)	7·1	3·9		
Specific surface area (m^2/g)	3·0	1·9		
Samples				
Pressing rate (arbitrary units)	1·0	1·0	1·3	1·3
Relative green density (%)	65	61	72	70
Relative nitrided density (%)	76	69	82	77
Bending strength (MPA)	258	146	307	175
Weibull modulus	23	12	19	11

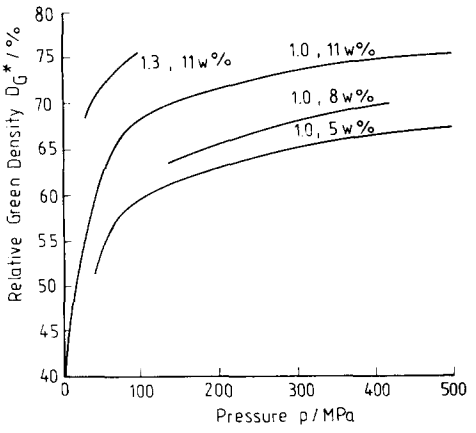

Fig. 2. Densification in die pressing, parameters attached to the curves denote pressing rate (arbitrary units) and percentage of siloxane additive.

for machining is reached after curing for 2 h at 200°C in air. Without a degassing treatment the cured samples were nitrided under equal conditions for 83 h up to 1450°C, in a mixture of $N_2/H_2 = 90/10$.

The RBSN properties obtained in this way are listed in Table 1. Taking into account the information contained in Fig. 4 (see Section 3), it can be stated that there is a linear relation between the densities of green and nitrided samples. The factor of proportionality was found from a larger set of data as 1·58, which deviates from the theoretical value of 1·665. The residue remaining after the pyrolysis of siloxane in the nitridation process (*c.* 40 wt% of the additive) does not seem to influence this factor, as can be concluded from the slope of the experimental curve, which coincides with that found by Mangels (mentioned in Ref. 4). Bending strength and Weibull number do not seem to be significantly related to the green density. These quantities are governed by the powder properties, as grain size distribution and grain shape. Strength turned out to be essentially influenced by the pressing rate. The use of siloxane is a precondition for increasing the pressing rate. The existence of these relations is the basis for the efforts to improve strength by means of methylphenylsiloxane.

Further it was investigated to which degree the mechanical properties could be improved also by infiltration of the green samples by siloxane. The optimum values of Table 1 may be roughly regarded as the largest improvement which can be achieved in this way.

3 Siloxane as an Infiltrating Substance

Infiltration is a well-known method for modifying the properties of porous ceramic and powder metallurgical materials.[5] Although the open porosity consists of a multiply connected network, the infiltration process can be approximately analysed by means of a capillary tube model. The flow of liquid into the tubes is governed by three forces: the applied pressure pushes the liquid in; surface tension either pulls in or pushes out, depending on whether the meniscus is concave or convex; and viscous shear stress limits the flow rate. The combined action of these forces results in a square root law of penetration depth versus time:

$$l = r \cdot \sqrt{\frac{t}{8\eta}\left(\frac{2\sigma\cos\theta}{r} + p_a\right)} \qquad (1)$$

where r = radius of capillary tube, σ = surface tension, η = viscosity, p_a = applied pressure, and θ = wetting angle.

The present infiltration experiments were performed by submerging the samples in the liquid substance at 80°C for 1 h under three different pressure regimes:

(1) 5 mbar to remove air from pores, then atmospheric pressure.
(2) 5, 10 and 15 bar nitrogen.
(3) Combination of (1) and (2).

The other parameters were kept constant. Outgassing removes the air from the pores which otherwise is trapped and compressed by the penetrating liquid and thus precludes thorough infiltration. For a first estimate of the effect of infiltration, green samples pressed from the powder Sil with 39% porosity (see Table 1) were infiltrated and subsequently cured at 200°C in air.

Figure 3 compares the pore size distributions before and after infiltration under a pressure of 15 bar and subsequent curing. It is seen that pores with radii above 400 nm, for instance, which make 80% of the total pore volume, are reduced to 10% after infiltration.

The reduction of porosity from 0·23 cm^3/g to 0·03 cm^3/g means that, after infiltration and curing,

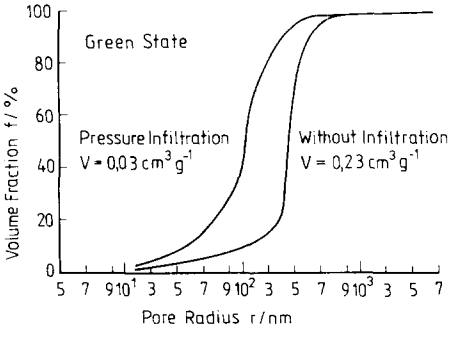

Fig. 3. Effect of siloxane infiltration on pore size distribution.

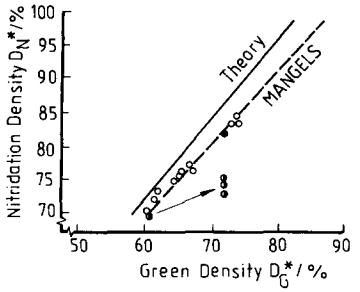

Fig. 4. Effect of siloxane infiltration (indicated by arrow) on green and nitrided density, compared with non-infiltrated samples.

the original pore volume is nearly completely filled with siloxane resin.

The samples were annealed at temperatures up to 600°C in flowing air for thermal decomposition of the resin, and then nitrided. Figure 4 compares the infiltrated and subsequently nitrided green samples with those of RBSN without additive. Starting from a low level, the green density is considerably increased by infiltration (see arrow). Subtracting the volatile fraction from the green density, i.e. taking into account only the 40 wt% residue after baking, would give a 64% green density for the infiltrated samples. Thus the three semi-black dots would be shifted to the left such that they would be placed among the other experimental dots which agree well with the results found by Mangels, represented here by the dashed line.

Because of a non-optimized thermal decomposition procedure, small cracks were formed at temperatures up to 600°C. Therefore the improvement of properties did not show up in the bending tests. The products of decomposition and other reactions change the composition of RBSN in a way not completely understood.

As seen from Table 2, infiltration considerably increases the carbon and oxygen content. As a consequence, a strong silicon oxynitride peak is found by X-ray diffractometry. Silicon carbide was not found, although expected. The content of α-phase increases as a result of the reaction of the siloxane, which is usually thought to influence the properties of RBSN favourably.

The effect of siloxane infiltration on materials properties is seen from Table 3. The density is correlated to the degree of infiltration of the green Sil samples. Open porosity is reduced by infiltration while closed porosity is virtually unaffected. Hardness seems to be correlated with total porosity. Fracture mechanical considerations suggest that the ratio between open and closed porosity may be a parameter governing fracture toughness. Infiltration under low vacuum and subsequently applied pressure reaches practically complete filling of the pores. Therefore the samples treated in this way indicate the ultimate improvement attainable by one-fold infiltration.

Data characterizing the pores are compiled in Table 4. They were obtained from crushed samples by the conventional mercury method. The green samples were cured and thus the siloxane was in the solid state. Obviously infiltration reduces the pore size. In nitriding the infiltrated samples, thermal

Table 2. Chemical and X-ray analysis of nitrided substances

	C (*wt%*)	*O* (*wt%*)	α (%)	β (%)	*Other*
RBSN from non-infiltrated green sample	1·9	2·6	56	44	Si_2ON_2 (trace)
RBSN from vacuum-infiltrated green sample	4·0	6·2	76	24	Si_2ON_2 (trace)
Nitrided methylphenylsiloxane	34–38	9–13	Small peak reflex	—	SiC β-SiO_2

Table 3. Properties of RBSN samples

	Powder	D_N (g/cm^3)	P_o (%)	P_c (%)	*HVT* (*GPa*)
Non-infiltrated	Sil	2·19	21	9	2·1
Vacuum infiltrated	Sil	2·32	19	7	4·8
Pressure infiltrated	Sil	2·36	16	9	5·0
Vacuum/pressure infiltrated	Sil	2·40	14	9	7·4
Non-infiltrated	S/M	2·63	4	13	7·5

D_N, nitrided density; P_o, open porosity; P_c, closed porosity; HVT, Vickers hardness.

Table 4. Characterization of pore structure

	Pore radius r_{50} (nm)	*Pore surface (m^2/g)*	*Pore volume (cm^3/g)*
Non-infiltrated, green nitrided	428	3·4–0·9	0·23
	101	4·4–2·8	0·11
Pressure infiltrated, green nitrided (15 bar, 80°C, 1 h)	124	0·5	0·03
	68	2·6	0·06

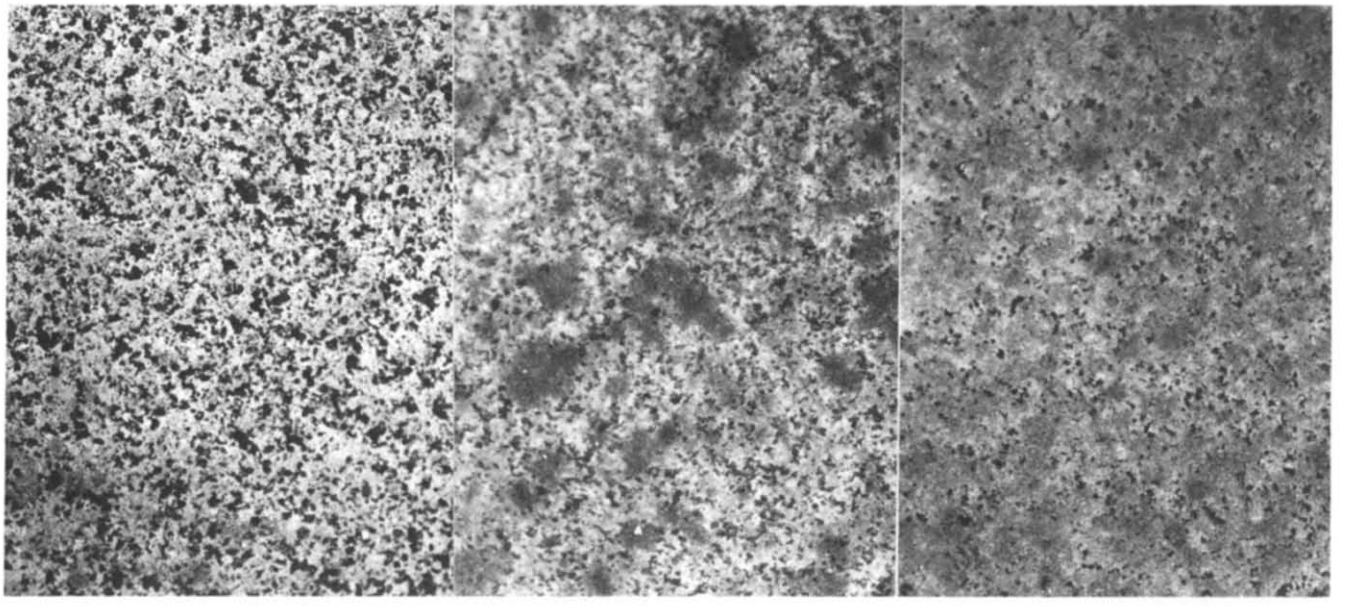

Fig. 5. Effect of siloxane infiltration on pore structure of nitridized samples: (a) non-infiltrated; (b) vacuum infiltrated; (c) pressure infiltrated.

decay of the polysiloxane seems to produce smaller pores, as suggested by the last line in Table 4. The changes of the pore system derived from porosimetry data are also seen directly from photographs as in Fig. 5: infiltration leads to smaller and less irregular pores. As expected from a fracture mechanical point of view, this results in higher hardness, as seen in Fig. 6.

Obviously, vacuum/pressure infiltrated samples from Sil powder reach the hardness level of samples from silicon powder S/M, though their density is lower. Hardness increases by a factor 3·5 with respect to non-infiltrated samples.

The applied Zwick hardness testing device provides a hardness number derived from penetration depth, which is denoted here by HVT. In addition to hardness, the device provides a number characterizing the elastic recovery after unloading. This number, denoted here by R, seems to be based on the belief that the size of the indent reduces strongly in the unloading process. This incorrect notion arose from the fact that the indent size found after unloading is much smaller than the apparent indent size derived from the assumption that the measured penetration path of the indenter equals the depth of the indent. Nevertheless, the number R is useful for deriving the elastic modulus from it. This is done by means of formulae discussed in Refs 6 and 7 relating the depth of the plastic indent, δ_p,and the elastic

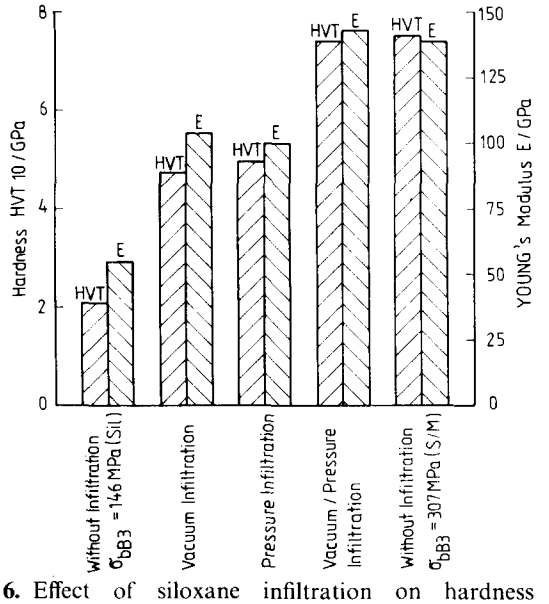

Fig. 6. Effect of siloxane infiltration on hardness and Young's modulus.

deflection, δ_e, to hardness, H, and Young's modulus, E. L is the applied load.

$$\delta_p = 0{\cdot}194\sqrt{L/H} \quad \delta_e = 0{\cdot}58\frac{1-\nu^2}{E}\sqrt{L\cdot H} \quad (2)$$

Note that the elastic deflection under load equals the back deflection in the unloading process, to a first approximation. Since the dependence on Poisson's number, ν, is rather weak, for simplicity, use can be made of the fact that ν is around 0·25 for most ceramics. By taking into account a small pre-load, L_0, as applied in the hardness test, one obtains the hardness and Young's modulus from the quantities provided by the testing device, HVT and R, in the following way:

$$H = \frac{\mathrm{HVT}}{1-R}$$

$$E = 2{\cdot}68\frac{\mathrm{HVT}}{1-R} \times \left(\frac{1}{(1-\sqrt{1-R})(1-\sqrt{L_0/L})} - 1\right) \quad (3)$$

Whereas HVT and the ill-conceived number R as provided by the testing device represent only some combination of hardness and modulus, the two quantities of interest are clearly separated in eqn (3).

As seen from the results in Fig. 6, Young's modulus as derived in the above way provides additional information independent of hardness. In particular, it is seen that the samples from Sil powder with 10 wt% siloxane reach a slightly higher modulus than the S/M samples, which indicates the high compactness of the material obtained by the sintering of siloxane-infiltrated samples.

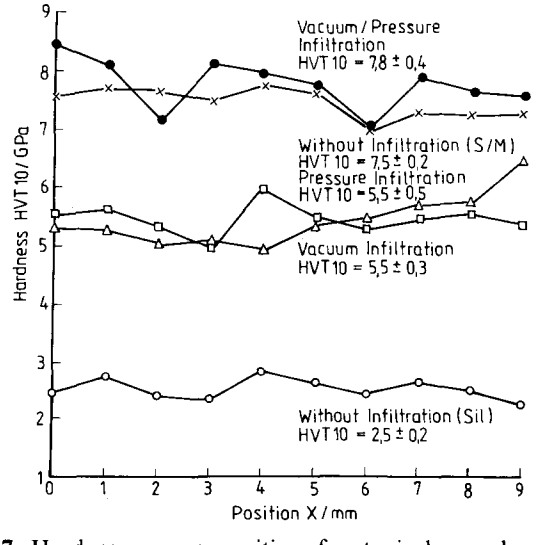

Fig. 7. Hardness versus position for typical samples from differently treated batches.

It is mentioned here that E derived in this way differs to some degree from the value obtained in the bending test. This is understandable in view of the fact that there is some difficulty involved in finding the position of the zero point of the unloading curve. Nevertheless, deriving Young's modulus from the penetration hardness test seems to provide another indicator, in addition to hardness, for the effect of the various infiltration techniques on the final properties.

The degree of inhomogeneity of the samples is seen in the plots of hardness versus position in Fig. 7. Vacuum infiltration decreases the relative scatter of hardness but pressure infiltration with air trapped inside increases it. Hardness measurement on cross-sections of vacuum-infiltrated samples indicates that the siloxane had penetrated into the interior of the samples.

4 Oxidative Decomposition of Methylphenylsiloxane

In order to avoid crack formation during pyrolysis of the polysiloxane, some knowledge on its temperature dependence is useful. In oxidative decomposition the siloxane resin releases mainly CO_2 and water vapour. The reaction is approximately described by

$$2(C_6H_5)_2(CH_3)_3Si_4O_{7\cdot5} + 40O_2 \rightarrow 30CO_2 + 19H_2O + 8SiO_2$$

The gases build up pressure within the pores and

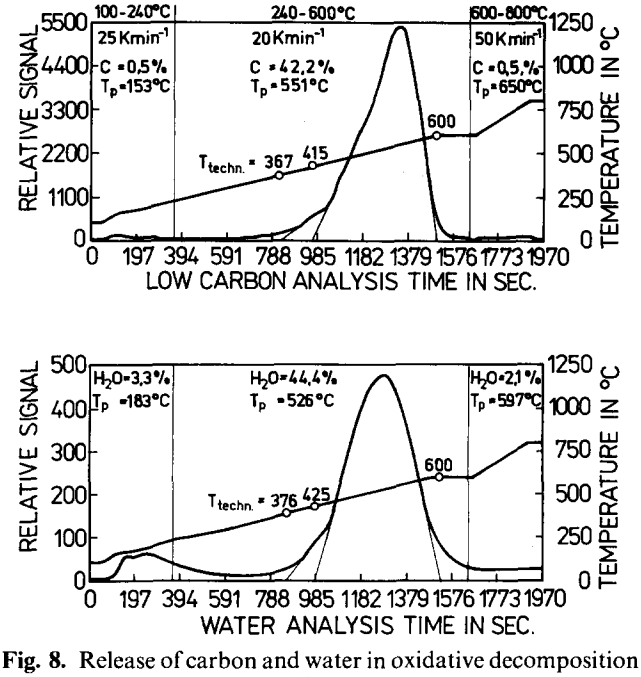

Fig. 8. Release of carbon and water in oxidative decomposition of methylphenylsiloxane.

give rise to cracking if released too quickly. The release rates of H_2O and CO_2 while heating up the sample are seen in Fig. 8. Even after baking at 600°C in air and subsequent nitridation, 4 wt% carbon remain in RBSN. Residual carbon and oxygen form carbide and oxide phases which are difficult to trace, probably because of their fine dispersion. Obviously, defects will most likely form in that temperature region where there is intense gas release. By measuring the amount of CO_2 and H_2O and also by thermogravimetry this region has been localized between 400 and 600°C (see Fig. 8). By reducing the heating rate within this region, crack formation during pyrolysis can be avoided. This has been found to result in higher hardness and is expected to favourably affect strength and fracture toughness, too.

References

1. Tank, E. & Gasthuber, H., Verfahren zum Herstellen von Werkstücken aus Siliziumnitrid, German Patent DE 2650083-A1, 30 October 1976.
2. Wynne, K. J. & Rice, R. W., Ceramics via pyrolysis. *Ann. Rev. Mater. Sci.*, **14** (1984) 297.
3. Seybold, M. & Greil, P., Composite ceramics from polymer–metal mixtures. In *1st European Conference on Advanced Materials and Processes*, Aachen, 1969, 614–47.
4. Wötting, G. & Ziegler, G., Dichtes Siliciumnitrid. I: Grundlagen, Herstellung, Eigenschaften und Anwendung. *Sprechsaal*, **119** (1986) 555–61.
5. Schatt, W., *Pulvermetallurgie, Sinter- und Verbundwerkstoffe*. Deutscher Verlag für Grundstoffindustrie, Leipzig, 1985, p. 408.
6. Weiss, H.-J., Krell, A. & Müller, B., Comparison of Vickers hardness numbers VH and LVH in the case of alumina and doped sapphire. *Phys. Stat. Sol. (a)*, **93** (1986) 509–14.
7. Weiss, H.-J., On deriving Vickers hardness from penetration depth. *Phys. Stat. Sol. (a)*, **99** (1987) 491–501.